

# Experimental and Numerical Investigation of the Effect of Mooring Stiffness on the Behaviour of $\Pi$ -Type Floating Breakwaters

Piero Ruol, Luca Martinelli, Paolo Pezzutto  
ICEA Department, University of Padova  
Padova, Italy

## ABSTRACT

Floating breakwaters (FBs) are suited to protect small marinas in mild sea conditions (wave periods up to 4 s and wave heights smaller than 1.5 m). Several companies in the world provide a very effective typology, a concrete rectangular caisson with two vertical plates protruding downwards from the sides. As these shapes resemble a  $\Pi$ , they are referred to as  $\Pi$ -type FBs.

In a previous paper, the Authors proposed a new formula for the transmission coefficient based on experiments on six different geometries of this type of FBs, with mass varying from 16 to 76 kg (representing prototypes at different scale, up to 130 tons), all anchored with chains. The formula identifies a key non-dimensional parameter as essential to describe the transmission phenomenon.

The aims of this paper are to investigate on the effect of the mooring stiffness, since the degree of restraining on the floating bodies is expected to alter significantly the FB's efficiency.

For this purpose, new experiments were recently carried out in a wave flume on FB anchored with piles and tethered with elastic lines, and an exploratory analysis is performed by means of simplified numerical simulations.

Based on these investigation, a second non dimensional parameter ( $d/h$ , i.e. draft over water depth) is identified as essential to predict whether lower transmission is obtained with a larger or a lower mooring stiffness. Only qualitative predictions are anyway proposed.

**KEY WORDS:** Design formula; Floating Breakwaters; Mooring system; Physical model tests; Wave transmission.

## INTRODUCTION

Floating structures are frequently used to protect coastal areas (lakes, open seas in mild wave conditions) or delicate ecosystems (lagoon marshes, tidal flats, etc), against wind or ship generated waves.

One of the advantages of floating structures is that their efficiency is almost independent from tide and, consequently, to sea level rise.

Furthermore, the environmental impact is low, the building and removal costs are small, the time required for installation is short and there is a possibility to rearrange the modules and/or to reshape the layout accommodating future modified uses.

A growing number of companies in Italy (Ingemar, AC Marine, Sistema Walcon, Martini Alfredo) and abroad (e.g. Archimedes Marinas, Greece; SF Marina, Sweden; Bellamer, Finland) provide concrete floating breakwaters (FBs) of patented shapes.

Each company provide more than one FB model. The larger ones are suited to protect the marinas from longer waves.

Examples of such models are (Cove, 2008):

- Ingemar (Italy), Type FCA 20x6, approx. 20x6 (160 tons)
- SF Marina (Sweden), Type SF 500, approx. 20x5 (60 tons)
- AC Marine (Italy), OSBW01, approx.. 20x4 (40 tons)
- Bellamer (Finland), Type 180, approx. 20 x 3

The geometries of the FB models are similar and in fact they may be considered of the same typology. The common feature is the presence of two vertical plates protruding downwards from the sides. The plates may be observed for instance in Figs. 1 and 2. Several other patented FB models could be presented, all characterized by the presence of the vertical plates. As the shape of these FB resemble the Greek letter  $\Pi$ , they are referred to as  $\Pi$ -type FBs (e.g. Gesraha, 2006).

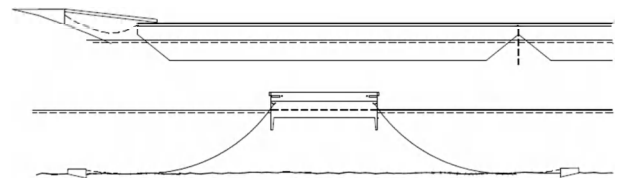


Fig. 1. breakwater  $\Pi$  type  
SF 300-SF 400 – SF 500 (SF Marina)



Fig. 2. Breakwater  $\Pi$  type  
(Martini Alfredo)

The recognized success of the  $\Pi$ -type FB proves that this typology is considered to perform very well. The efficiency, or performance, of a floating breakwater is mainly expressed in terms of the transmission coefficient  $k_t$ , defined as the ratio between transmitted and incident wave height. Clearly the larger the draft of the FB, the smaller the wave transmission on the lee side (Cox et al., 2007; Peña et al., 2011). Therefore, the advantage of the vertical plates is to increase the draft in an economical way, similarly for instance to the T-shape FB (Blumberg and Cox, 1988; Neelamani and Rajedran, 2002). Another reason to have a pair of plates beneath the FB is to confine a certain volume of fluid, forcing it to follow the displacements of the floating body, so that the added mass is increased with respect to the rectangular caisson of equivalent mass. It will be shown that larger mass and therefore larger eigenperiods, induce less transmission. Anyway, if the two attached plates are too long, they may behave as radiating wave sources, decreasing therefore FB efficiency in short wave sea states.

The efficiency of  $\Pi$ -type FBs moored with chains has been studied by Ruol et al. (2012), who propose a predictive formula given in the following Section. The formula does not account for the effect of the mooring system itself, although it is well known that the restraining mechanism affects the global performance. For instance a recent investigation on cylindrical FBs (Ozeren et al., 2011) proved that horizontally restrained models performed better than vertically restrained models.

The aim of this work is to investigate on the effect of the mooring system type and stiffness in terms of wave transmission, by means of numerical and experimental results.

In the next Section, the results of experiments on FB moored with different systems are presented. Then, numerical simulations are described representing different stiffness conditions: FB free to move in all directions (loose chains), free to oscillate vertically (piles), fixed (tethered).

Final comments are drawn on the basis of these analyses.

#### THE FORMULA DEVELOPED FOR COMPLIANT MOORING SYSTEM

Ruol et al. (2012) proposed a formula that is a modification of the Macagno analytical relation.

The Macagno relation is given by the following Eq. (1):

$$k_{tM} = \frac{1}{\sqrt{1 + \left[ kw \frac{\sinh kh}{2 \cosh(kh - kd)} \right]^2}} \quad (1)$$

This relation is valid for a rectangular, fixed and infinitely long FB with draft  $d$  and width  $w$ , subject to regular waves. In Eq. (1)  $h$  is the water depth and  $k$  is the wave number relative to a regular wave. For irregular waves, where  $T_p$  is known, we evaluate the wavenumber assuming an equivalent period  $T = T_p/1.1$ .

Since Macagno's relation is based on linear wave theory in absence of displacements and dissipations, it does not predict accurate results. Furthermore, it is not meant to be applied to floating  $\Pi$ -type FBs.

Ruol et al. (2012) introduce a non-dimensional parameter  $\chi$ , that interprets the ratio between the peak period of the incident wave  $T_p$  and the natural period of the heave oscillation  $T_{heave}$  (in absence of mooring):

$$\chi = \frac{T_p}{2\pi} \sqrt{\frac{g}{d + 0.35w}} \quad (2)$$

The symbol  $\chi_m$  is used if the mean wave period  $T$  is used rather than the peak wave period  $T_p$ .

The method proposed by the Authors consists in evaluating the transmission coefficient  $k_t$  multiplying the Macagno's relation by a function of  $\chi$ .

The proposed transmission coefficient is written in the form of Eq. (3):

$$k_t = \beta(\chi) k_{tM} \quad (3)$$

$\beta$  is given by the following expression:

$$\beta = \frac{1}{1 + \left( \frac{\chi - \chi_o}{\sigma} \right) e^{-\left( \frac{\chi - \chi_o}{\sigma} \right)^2}} \quad (4)$$

where  $\chi_o = 0.7919$  (with 95% confidence interval 0.7801, 0.8037) and  $\sigma = 0.1922$  (0.1741, 0.2103). Eq. 4 is valid in the range  $\chi \in [0.5; 1.5]$ .

Note that Eq. 4 is merely a fitting of the experimental results. The core of the proposed method is given by Eq. 3, that assumes  $\chi$  as the most relevant variable of the process beside the prediction based on Macagno's relation.

The fitted results derive by several physical model tests carried out on the 6 structures described in Table 1. The first four structures are shown in Fig. 3, the fifth is shown in Fig. 4. The last one is similar to the fifth.

In particular, Fig. 4 shows that the wave approaching from the left (or incident) side is attenuated, so that on the right (or lee) side, a very small wave is visible.

All devices were moored with 4 chains, with submerged weight of approx. 70 g/m, anchored at a distance equal to twice the water depth ( $h=0.5$  m). The initial pretension is very low, equal to the total chain weight. In shallow waters, chains may become fully extended in case of large waves. The sharp impact load that develops in case the chain is fully extended was studied in Martinelli et al (2008).

Fig. 5 shows all the results of the  $\Pi$ -type floating breakwaters tests (with chain mooring configuration) plotted according to the proposed method (Eq. 3). Fig 6 shows the good agreement between the formula and the results. The formula was fitted to cases with incident waves smaller than the freeboard ( $F_r$ ). Comparison with literature data also showed good agreement, at least for small incident wave heights. In case of large waves, the transmission is seen to be slightly under-predicted for small  $\chi$  and over-predicted for large  $\chi$ .

Tab. 1. Structures tested in the wave flume.

Model code	Weigth (kg)	Width w (m)	Heitgt hs (m)	Draft d (m)	Mooring type (m)
Sc0c07kg	7.25	0.20	0.120	0.065	Short chain
Sc0c16kg	16.20	0.25	0.100	0.100	Short chain
Dc0c32kg	32.00	0.50	0.150	0.100	Short chain
Dc0c56kg	56.30	0.50	0.283	0.178	Short chain
Dc0c76kg	76.30	0.50	0.283	0.238	Short chain
Mc0c76kg	76.30	0.50	0.343	0.238	Short chain



Fig. 3. Four structures tested in the wave flume.

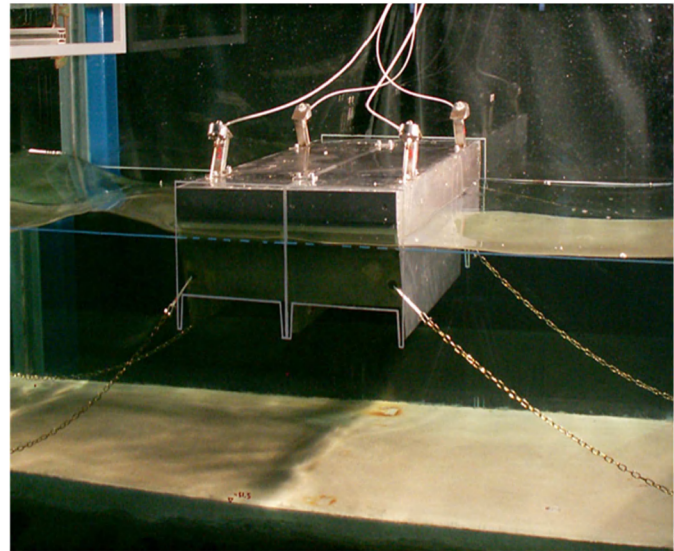


Fig. 4. Example of large breakwater tested in the wave flume of Padova University.

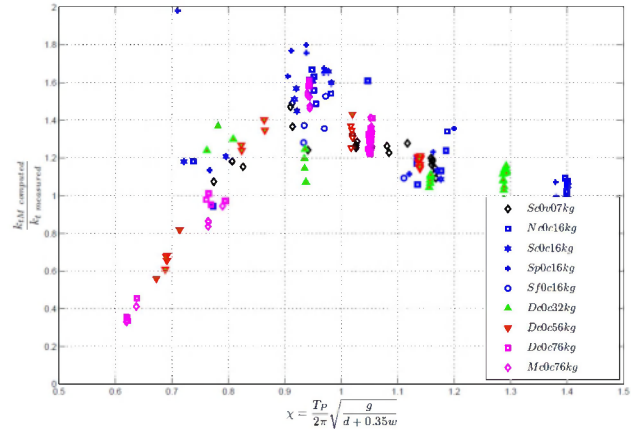


Fig. 5. Transmission results plotted according to Eq. 3.

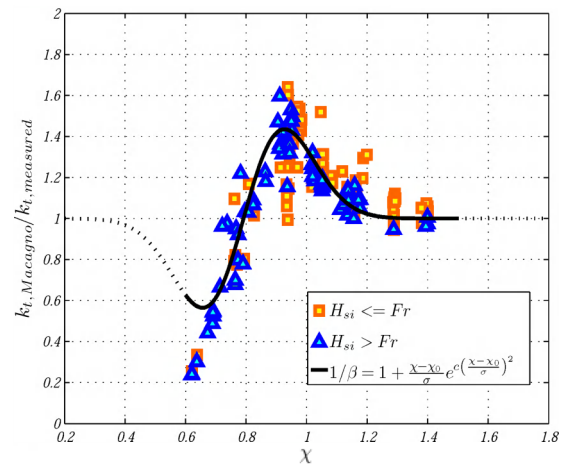


Fig. 6. Comparison of the proposed equation (Eqs. 3 and 4) with  $\Pi$ -type floating breakwaters.

## MODEL TESTS

New tests were carried out in the Wave flume of Padova University in order to study the effect of different mooring systems in terms of effectiveness to reduce waves. The procedure followed to carry out the tests is basically the same adopted in previous tests. Fig. 7 shows the experimental set up. Two arrays of four resistive type wave gauges are used to separate the incident and reflected waves. Loads on the chains are measured by 4 full bridge strain gauges. Wave gauges data are sampled at 20 Hz, load cells ones at 100 Hz. Water depth is 800 mm and the bed is flat under the device. An absorbing beach in the rear side is used to dissipate the transmitted energy. Several irregular wave conditions (JONSWAP spectra with 3.3 shape factor) were generated (forming a grid with different periods and different wave steepness), using the paddle in piston mode and an active wave absorption system.



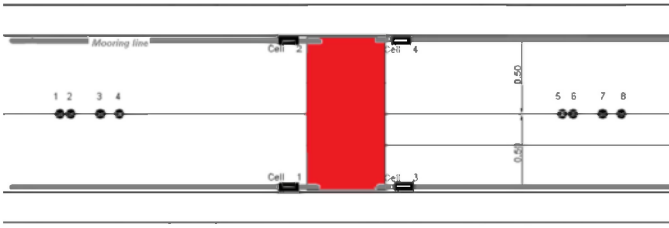


Fig. 7. Top view of the wave flume in correspondence of the test section, with the wave gauge and load cell position.

The new tested structures have code dt0c15kg, dc0c15kg and sp0c12kg. The main characteristics are listed in Tab. 2.

Three different mooring system were used:

- a very stiff tethered system (Fig. 11), with elasticity similar to that of polyester lines (3% elongation at full stress). Tethered mooring line is generally formed by a pre-tensed elastic line that should remain always in tension during the whole wave cycle.
- loose chains; chains have submerged weight of 70 g/m, length is 4 m, i.e. 5 times the water depth. Initial pretension is approximately 70 g. The resulting initial mooring stiffness is low and no shocks have been observed.
- piles (connection of typical prototype setup, shown in Fig. 8, was reproduced by means of special Teflon rings, shown in Figs. 9 and 10);

Tab. 2. New tested structures (two geometries)

Model code	Weigth (kg)	Width w (m)	Heitgt hs (m)	Draft d (m)	Mooring type (m)
dt0c15kg	15.0	0.3	0.12	.084	Tethered
dc0c15kg	15.0	0.3	0.12	.084	Loose chains
sp0c12kg	12.5	0.2	0.10	.070	Piles

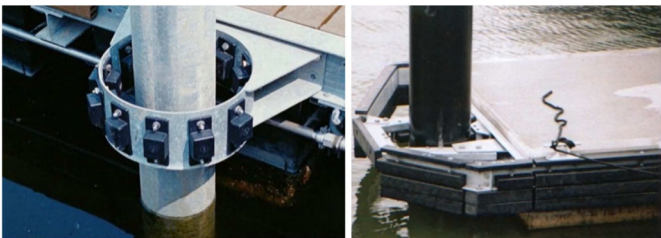


Fig. 8. Example of pile connections. Martini Marina (Left)- Archimedes Marinas (Right)



Fig. 9. Detail of pile connection. Physical model test

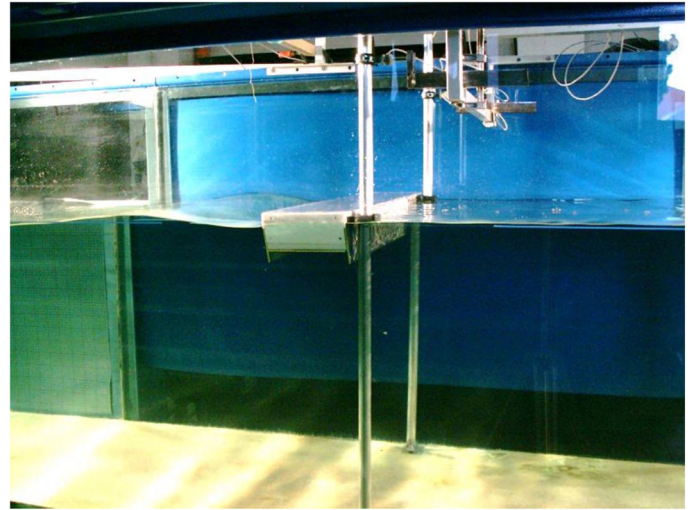


Fig. 10. Piles

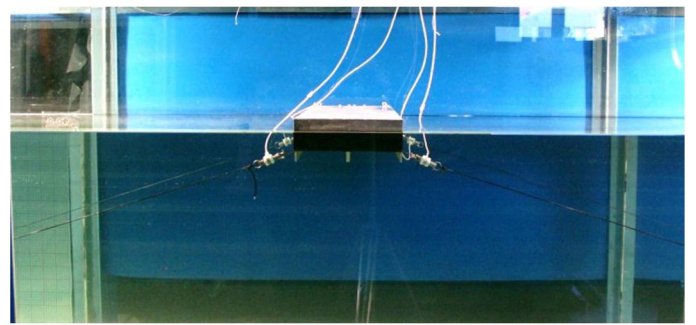


Fig. 11. Stiff tethered system

## MODEL TEST RESULTS

A qualitatively different dynamic behavior was observed for the three mooring system types:

- in presence of tethered lines, the movements were quite less ample (50%) compared to the chain mooring system. This was certainly due to the much larger material stiffness of the lines compared to the geometrical stiffness of the chain (due to the catenary shape). An unexpectedly large damping was also noticed, since, after displacing by hand the FB from the static position in calm waters, the initial configuration was restored after just 2-3 oscillations. This behavior may be a model effect, since no general specifications on prototype damping of tethered lines is available.
- in presence of loose chains, the FB could move rather freely, and only second order drift was avoided;
- in presence of piles, the PF could move according to 2 Degrees of Freedom (DoF), i.e. heave and roll; rotations were allowed up to a certain extent, since the lower part of the FB would hit the pile in case of excessive tilting;

Fig. 12 shows a summary of the results for the three mooring systems, in terms of transmission coefficient. Results relative to the mooring loads are also available, although out of the scope of this investigation. In a quite large range of wave periods, FBs with piles behave much better than the other solutions. Loose chains appear to be the least effective case.

Points in Fig. 13 are the experimental data presented according to the method proposed by Eq. 3, i.e. dividing  $k_{IM}$  obtained with Macagno

formula by the measured  $k_t$  and plotted as a function of  $\chi_m$ . The dotted lines are obtained with the numerical approach described in the next paragraph.

It may be noticed in Fig. 5 that the case with loose chain (squares) agree with predictions based on Eqs. 3 and 4. In terms of transmission coefficient, piles and tethered models appear to be overestimated by 25-50%, or else we should say that the measured transmission is significantly lower than predicted by the formula suited to a compliant mooring system (Eqs. 3 and 4).

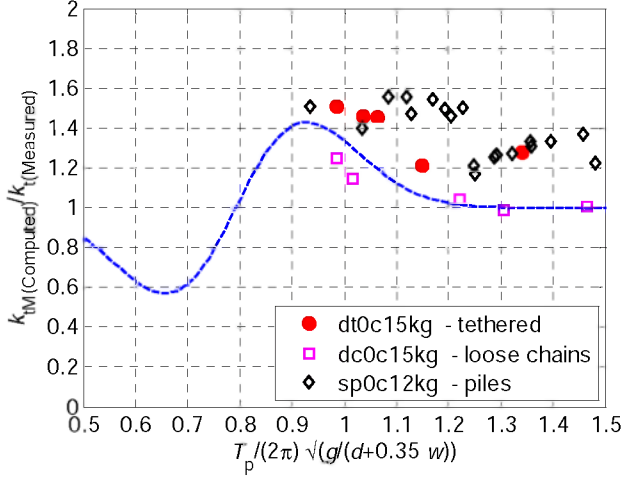


Fig. 12. Model test results, plotted vs the proposed non-dimensional parameter  $\chi$ .

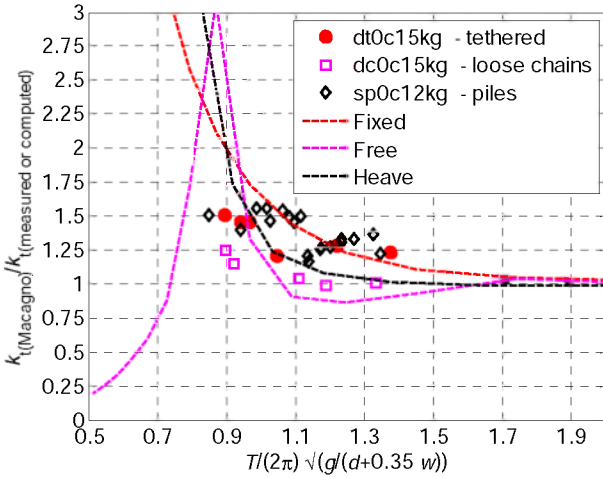


Fig. 13. Model test results and prediction of the proposed method (Eq. 3). Experimental values are plotted using the measured mean period  $T_m$ .

## NUMERICAL APPROACH

A first order potential flow numerical model is set up to study the FB dynamics in the wave flume. Since only heave, sway and roll are allowed in the flume (due to the presence of the side walls), the problem is essentially 2D.

A code based on the Finite Element Method (FEM) has been developed. The 2D domain is divided into a large number of nodes and a system of equation is set up that accounts for all interactions between nodes, storing the coupled terms into a large matrix. A well-known

characteristics of this kind of potential problem is that many elements of the matrix are zero. In fact, memory limitations generally suggest to use Boundary Element methods instead. By means of the Green function, the 2D problem could be further reduced into a 1D numerical problem. The Boundary element method allow to produce a single "full" vector that only keeps the important information, much more compact.

In practice, however, the advantage in memory allocation is much smaller than it could appear, since the matrix is anyway stored in a sparse way, where only the non-zero elements are memorized. Furthermore, for the investigated case the water depth is shallow (and the bed has in some cases a very mild slope) so that the Green function becomes somewhat tedious to program. In conclusion it was decided to model the whole 2D problem with a FEM solver, and describe the potential problem in a straightforward way.

The linearized problem is well described in many textbooks. The procedure suggested by Fugazza and Natale (1988) was used, since it contains a simple correction term that forces energy conservation. As explained in that paper, in absence of FB movements the diffraction problem correctly divides the incident wave energy into reflected and transmitted ones. In presence of radiated waves, an additional component of reflected and transmitted energy appear whereas, as a result of linearization, the scattered solution is not modified. As a consequence, the energy balance is no longer guaranteed. The simple suggested approach is to apply to all potential terms a weighted reduction coefficient that resets the balance.

The hydrodynamic load obtained with the linear potential approach is trivially proportional to the wave height, and varies with the incident regular wave period  $T$ . A range of values are considered, included between half and twice the natural period of the heave oscillation  $T_h$  (in 10 steps).

Three different types of mooring systems are numerically analysed, that resemble but do not completely simulate the real mooring constraint. They are termed as:

- 'Heave': a case where only vertical movements are allowed (resembling the case of Piles, although with some discrepancies as far as the real hinge, see Fig. 8, usually allows some roll oscillation, although with limited amplitude); in the simulations, surge and roll are frozen;
- 'Fixed': a case where all movements are frozen (resembling the case with tethered lines, where displacement are small since linear horizontal and vertical reaction allow only for small movements);
- 'Free': a case where a linearised spring system is modeled (resembling the case of chains, that provide a reaction with very low stiffness). The term free does not mean here that the FB is not moored, but that all movements are possible. The spring reaction is modelled assuming a linear spring coefficient due to an initial pretention of 100% of the total weight of the chain, as it happens in the physical model case. The obtained linearized stiffness is a very weak value allowing large movements. This simulation represents the case of a very compliant system where the mooring only absorbs the second order drift load. Application of a full non-linear approach was not carried out for simplicity. A more refined approach is on the other hand not justified, given the limited accuracy of the 1<sup>st</sup> order potential approach.

## COMPARISON BETWEEN SIMULATIONS AND MODEL TESTS

The first phase of the numerical investigation aims at defining the accuracy of the numerical model in case of II-type FB. For this reason, the structures studied in the laboratory were numerically simulated.

The numerical dataset simulates the 6 tests listed in Tab 1 and the 3 new ones listed in Table 2. For all tests, the transmission coefficient is derived for the "Heave", "Fixed" and "Free" case.

Fig. 14 shows a comparison between all the simulated conditions (points) and the prediction according to Macagno's relation, plotted vs  $\chi_m$ . Note that the  $\chi$  variable depends on the "peak" period of the incident wave. When results relative to regular and irregular waves are compared, such as in case of model tests and numerical simulations, the non-dimensional variable  $\chi_m$  is used.  $\chi_m$  is based on the mean period  $T_m = T_p/1.1$  in case of model tests, and the regular period  $T$  in case of numerical simulations. Similarly, the Macagno's relation is always computed for  $T = T_p/1.1$ .

The numerical and Macagno's prediction are not so different in case the II-type FB is constrained to be fixed.

It may be observed that, regardless of the different geometries of the structures ( $d/h$  values), the numerical results appear to have the same trend when they are plotted against the identified variable.

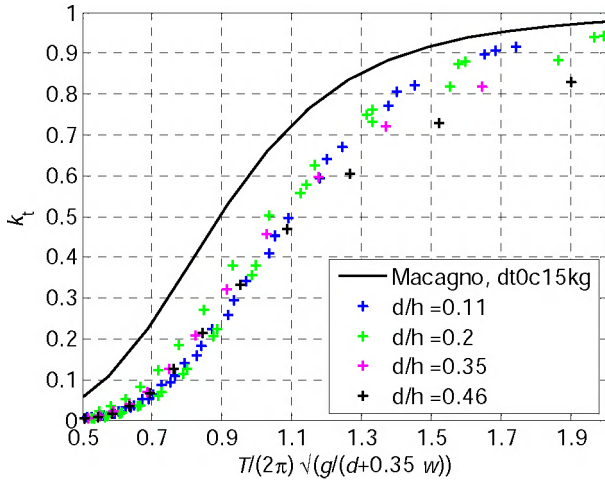


Fig. 14. Comparison between Macagno prediction (dotted lines) and runs of the numerical simulations for fixed structure (points).

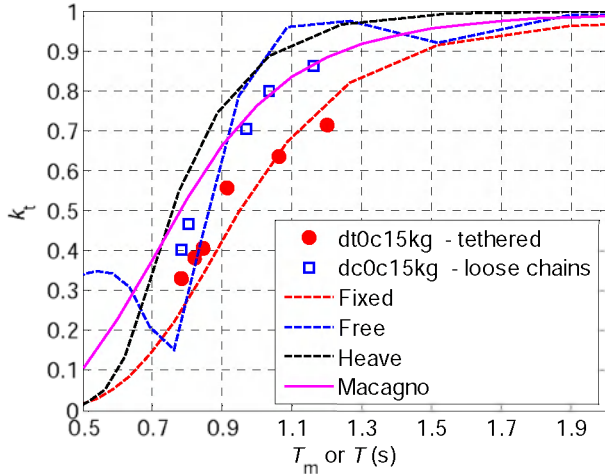


Fig. 15. Geometry defined by structure dt0c15kg. Comparison between Macagno and numerical model simulations (function of  $T$ ) and experimental results (plotted Vs the measured mean period  $T_m$ ).

The sensitivity of the numerical model to the type of mooring systems is investigated in Figs. 15 and 16.

Fig. 15 compares the Macagno's relation, the model prediction and the experimental results for one single structure ('dt0c15kg').

Fig. 16 compares the experimental  $k_t$  for the three different mooring system to the simulations based on the same geometries and associating (by means of the same color) the "Heave" simulation to the Pile restrained tests, the "Free" to the chain moored tests and the "Fixed" case to the tethered mooring system.

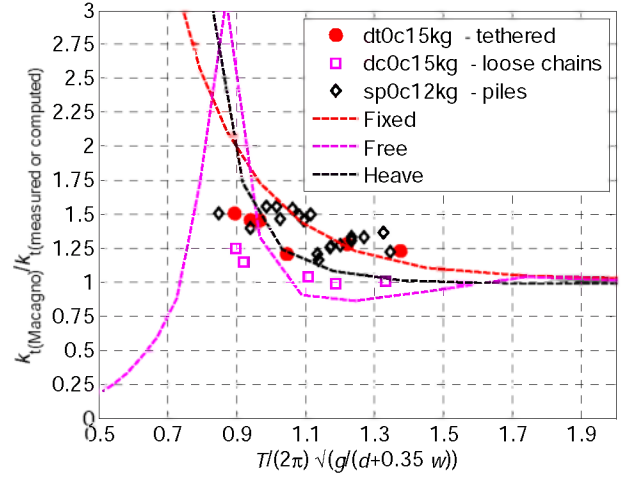


Fig. 16. Experimental and numerical results. Simulations relative to regular wave period  $T$  were associated to a peak period  $T_p = 1.1 T$ .

#### EXPLORATORY INVESTIGATION

The exploratory investigation on the mooring systems is obtained comparing the effect of the different numerical constraint types for 90 different geometries, characterized by:  $a/d \in [0.05; 0.75]$ ,  $w/d \in [0.2; 7.7]$ ,  $d/h \in [0.07; 0.9]$  where  $a$  is the vertical plate heights,  $d$  is draft,  $w$  is width,  $h$  is water depth.

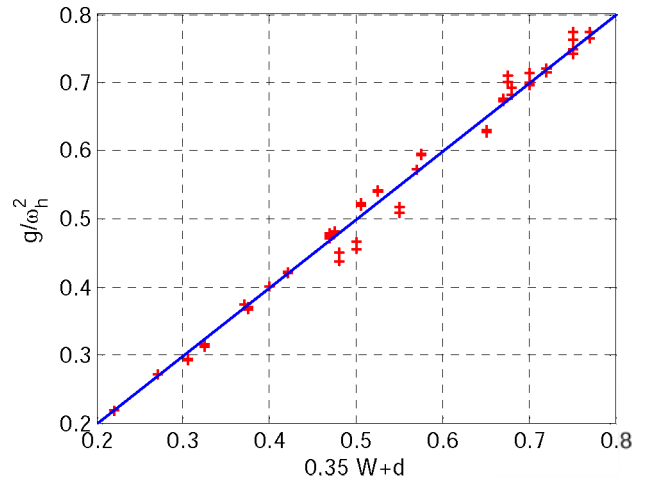


Fig. 17. Validation of the equation for the prediction of the natural period of the II-type FB.



Initially, the period of the heave natural oscillation is computed for all the structures. Interpretation of the  $\chi$  parameter as the ratio between the peak period and the natural period of the heave oscillation is based on the experimental fitting of the formula  $g/\omega_n = d + \alpha w$ , with  $\alpha = 0.35$  (for an infinitely long box type FB,  $\alpha = \pi/8 \approx 0.39$ ). Fig. 17 shows that the chosen value for  $\alpha$  is rather accurate in the whole range of simulated structures.

The numerical results are plotted as a function of the independent variable  $\chi_m$ . Figs. 18, 19 and 20 show the numerical results for different  $d/h$  values.

Structures have been grouped based on the non-dimensional parameter  $d/h$ , i.e. the ratio between draft and water depth. Higher values of this non-dimensional parameter are associated with lower transmission in the whole range of  $\chi_m$ . In the figures, the points relative to a particular FB geometry ( $a, w, d, h$ ) are connected by a line representing the typical structure behavior.

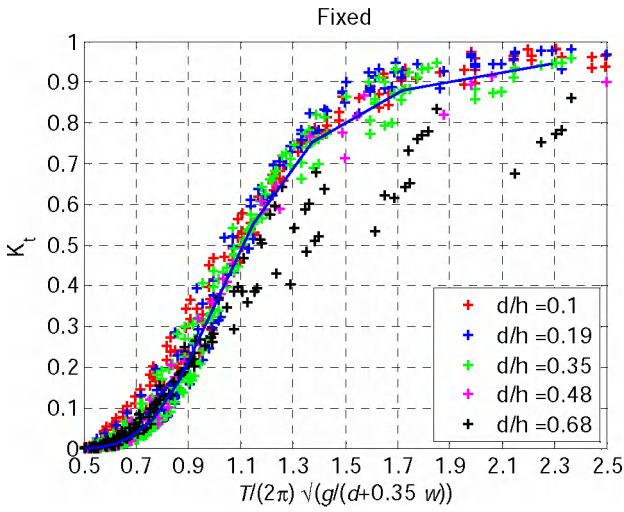


Fig. 18. Transmission for the simulated structures constrained to be "Fixed".

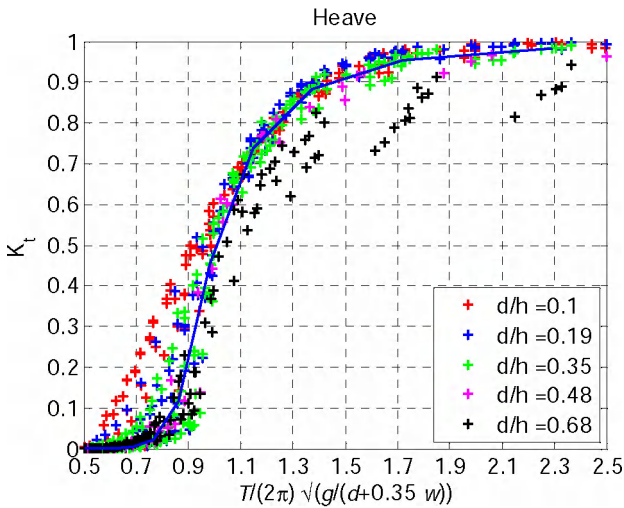


Fig. 19. Transmission for the simulated structures constrained to be "Fixed".

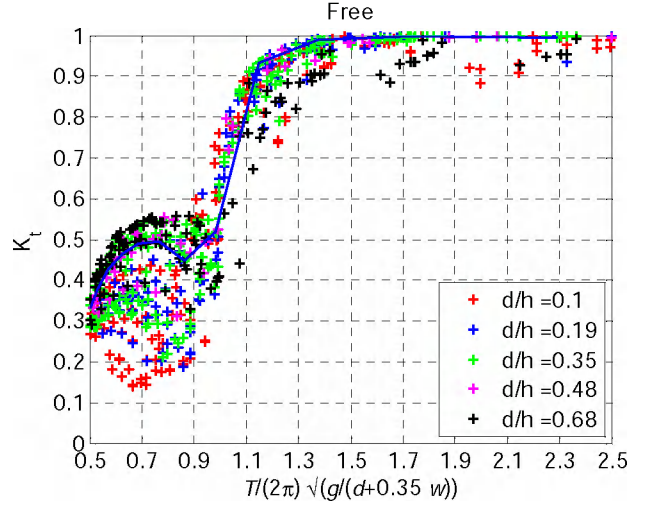


Fig. 20. Transmission for the simulated structures, anchored with very compliant chains.

Figs. 21, 22 and 23 show the effect of the type of constraint on the numerically calculated  $K_t$  values. They present the ratio between transmission coefficient relative to different types of mooring. Plots are organized with the same criterion used for Figs. 18, 19 and 20. It may be observed that the sensitivity to the type of constraint clearly depends on the ratio  $d/h$ .

From Fig. 21 it may be observed that – according to the numerical simulations – transmission in Fixed configuration is always lower than in Free configuration. Higher differences are observed for low periods and lower  $d/h$  values.

From Fig. 22 it may be observed that transmission in Heave configuration is even lower than in Fixed configuration when the wave period is lower than the natural period of oscillation, provided that the structure draft is sufficient ( $d/h > 0.1-0.2$ ).

When the draft is small ( $d/h < 0.1-0.2$ ) and the period of oscillation is close to the natural one, transmission in Heave is even larger than in Free configuration.

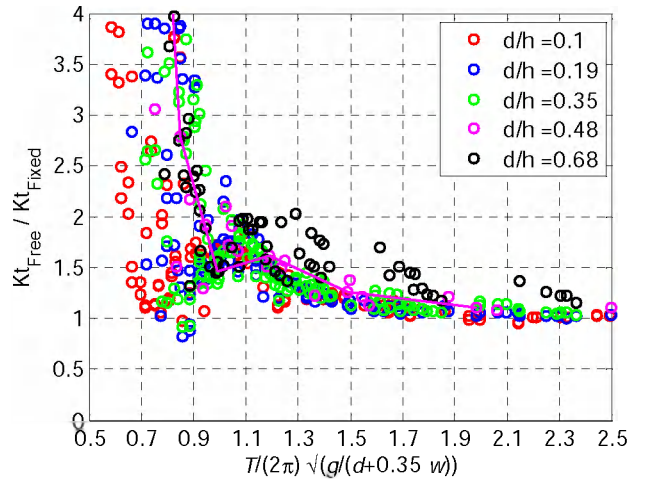


Fig. 21. Ratio of the transmission coefficient in Free and Fixed configuration.

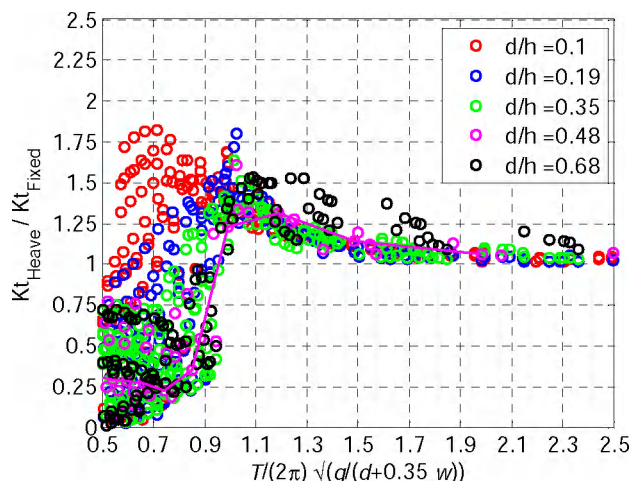


Fig. 22. Ratio of the transmission coefficient in Heave and Fixed configurations.

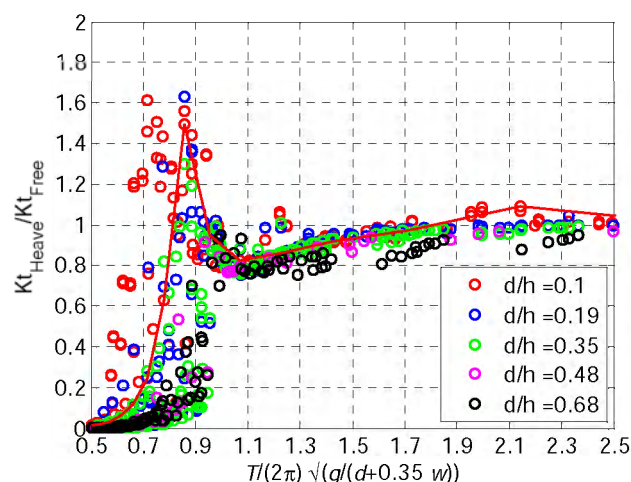


Fig. 23. Ratio of the transmission coefficient in Heave and Free configurations.

## CONCLUSIONS

The experimentally based equation by Ruol et al (2012) for the prediction of wave transmission relative to  $\Pi$ -types floating breakwaters (FBs) anchored with chains was presented.

New tests and numerical simulations were carried out aiming at defining the behavior of this type of FBs for different mooring systems. The tests have been performed in the wave flume of Padova University, Italy, on FBs anchored with loose chains, tethered lines and connected to piles.

2D numerical simulations considered FB fully constrained (Fixed, in order to roughly simulate tethered conditions), free to move vertically (Heave, simulating pile supports) and moored with loose springs (Free, simulating the chain mooring).

The investigation concluded that the most effective restraining system mainly depends on the range of periods of interest and on the ratio between draft and depth.

FBs moored with loose chains (Free) are less effective than tethered ones (Fixed) in almost all the investigated range (Fig. 21).

Considering wave periods smaller than the natural period of oscillation ( $\chi_m < 1$ ) and large drafts ( $d/h > 0.2$ ), pile supported (Heave) FBs perform better than tethered supported ones (Fig. 22).

For periods close to the natural period of oscillation and small drafts ( $d/h < 0.1$ ), chain moored FBs behave better than pile supported FBs (Fig. 23).

## ACKNOWLEDGEMENTS

The support of the European Commission through Contract 244104 THESEUS ("Innovative technologies for safer European coasts in a changing climate"), FP7.2009-1 Large Integrated Project, is gratefully acknowledged.

The Authors acknowledge also INGEMAR S.r.l. for providing information regarding their devices.

## REFERENCES

- Blumberg G.P., Cox R.J. (2000). *Floating breakwater physical model testing for marina applications*. PIANC-AIPCN Bull. n°63.
- Cove M. (2008). *A-Z guide to pontoon sand floating breakwaters*. Marina World, September/October 2008 No.49 Vol 9 Issue 1
- Cox R., Coghlan I., Kerry C.. (2007). *Floating breakwater performance in irregular waves with particular emphasis on wave transmission and reflection. energy dissipation. motion and restraining forces*. Proc. Coastal Str. '07, 1, 351-362.
- Fugazza M. and Natale L. (1988). *Energy losses and floating breakwater response*. Journal of Wat., Port, Coastal, and Ocean Eng., 114 (2), March, 1988.
- Gesraha Mohamed R. (2006). *Analysis of  $\Pi$  shaped floating breakwater in oblique waves: I. Impervious rigid wave boards*. Appl. Ocean Res., 28(5), 327-338.
- Martinelli, L., Ruol, P., Zanuttigh, B. (2008). *Wave basin experiments on floating breakwaters with different layouts*. Appl. Ocean Res., 30(3), 199-207.
- Neelamani S., Rajendran R.. (2002). *Wave interaction with T-type breakwaters*. Ocean Eng., 29, 151-175.
- Ozeren Y., Wren D. G., Altınakar M., Work P. A. (2011). *Experimental Investigation of Cylindrical Floating Breakwater Performance with Various Mooring Configurations*. J. Waterway, Port, Coastal, Ocean Eng. 137, 300-309.
- Peña, E., Ferreras J., Sanchez-Tembleque F. (2011). *Experimental study on wave transmission coefficient, mooring lines and module connector forces with different designs of floating breakwaters*. Ocean Eng., 38 (10), 1150 - 1160.
- Ruol P., Martinelli L., Pezzutto P. (2012). *Formula to Predict Transmission for  $\Pi$ -type Floating Breakwaters*. Journal of Wat., Port, Coastal, and Ocean Eng., in print - available online, doi:10.1061/(ASCE)WW.1943-5460.0000153.